

# A structural study of metastable tetragonal zirconia in an $\text{Al}_2\text{O}_3\text{--ZrO}_2\text{--SiO}_2\text{--Na}_2\text{O}$ glass ceramic system

G. FAGHERAZZI, S. ENZO

*Instituto di Chimica Fisica, Calle Larga S. Marta 2137, 30123 Venezia, Italy*

V. GOTTARDI, G. SCARINCI

*Instituto di Chimica Industriale, Via Marzolo 9, Padova, Italy*

The structural and microstructural properties (crystalline system at the beginning of crystallization, lattice disorder and crystallite size) of metastable zirconia have been studied by an X-ray line broadening analysis using simplified methods based on suitably assumed functions describing the diffraction profiles. Metastable tetragonal zirconia has been crystallized at 970, 1000 and 1050° C, respectively, starting from an  $\text{Al}_2\text{O}_3\text{--ZrO}_2\text{--SiO}_2\text{--Na}_2\text{O}$  glassy system with a chemical composition very close to that of well known electromelted refractory materials. In the present work we have definitely shown the presence, inside the crystallized zirconia phase, of internal microstrains having values ranging approximately between 2 and  $4 \times 10^{-3}$ . Moreover, we have confirmed the peculiar smallness in size of precipitated zirconia crystallites ( $\leq 200 \text{ \AA}$ ). Therefore, in the present system, the stabilization of the tetragonal form of  $\text{ZrO}_2$  with respect to the stable monoclinic one can be explained in terms of a contribution to the amount of free energy due to strain energy, in addition to the previously hypothesized surface energy. The observed strong line broadening for some samples treated at lower temperatures (970 and 1000° C) gives rise to an apparent cubic lattice pattern; but the asymmetry of each apparent single line masks unequivocally a tetragonal doublet. This latter conclusion disagrees with some hypotheses on the existence of a cubic metastable form of  $\text{ZrO}_2$  which could originate at the beginning of zirconia crystallization.

## 1. Introduction

In the present paper we describe the structural and microstructural properties of metastable zirconia in an  $\text{Al}_2\text{O}_3\text{--ZrO}_2\text{--SiO}_2\text{--Na}_2\text{O}$  glass ceramic system, its chemical composition being very close to the one of a well known electromelted refractory material.

The glass matrix was prepared according to previously published methods [1, 2] by applying a gelling process to a solution of the parent metallo-organic compounds and mildly heating the material up to about 900° C so that an homogeneous glass was formed. That method was extensively elucidated by Gottardi *et al.* [3] by differential thermal (DT), thermal gravimetric (TG) as well as by X-ray diffraction analyses for the present glass ceramic system. Fig. 1 shows the DT analysis

with an exothermic peak clearly appearing at about 940° C. That peak was ascribed to the zirconium dioxide crystallization in the metastable tetragonal form [4] which rearranges itself into the monoclinic stable form (baddeleyite) on increasing the annealing temperature up to 1500° C. Selective chemical analyses displayed a progressive, parallel, increase of the crystallization of the system, at the expense of the amount of glass phase [3].

At about 1150° C the monoclinic zirconia X-ray lines are clearly detectable together with those of mullite, while traces of corundum and zircon begin to become visible. At 1300° C the tetragonal metastable zirconia concentration has clearly decreased while the monoclinic one has correspondingly increased; mullite, corundum and

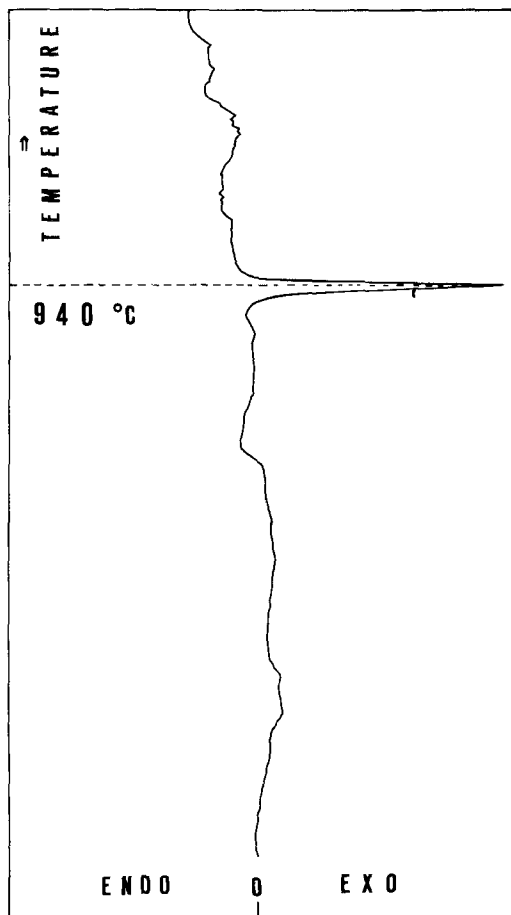


Figure 1 DT analysis of the  $\text{Al}_2\text{O}_3\text{-ZrO}_2\text{-SiO}_2\text{-Na}_2\text{O}$  glass ceramic system examined. An exothermic peak clearly appears at about  $940^\circ\text{C}$ .

zircon phases have also increased and this trend has grown stronger as the temperature has risen from  $1300$  to  $1500^\circ\text{C}$  (for some hours of isothermal annealing).

The material studied here is an interesting point of departure in preparing glass ceramics for high temperature use. In fact, the present preparation method permits one to obtain a much smaller glass phase than the one obtainable by the usual melting processes and with a negligible porosity. Moreover, several measurements (not reported here) have shown that the devitrification process occurs with a low density change (e.g. it varies from  $3.75 \pm 0.03$  to  $3.90 \pm 0.03 \text{ g cm}^{-3}$  for the series of eight samples examined here).

The possibility [3] of obtaining most of the zirconia, under certain conditions, in a tetragonally metastable form, results in a greater resistance to thermal shocks compared with the glass ceramics obtained by other melting processes.

We therefore decided to study the structural and microstructural properties of tetragonal metastable zirconium dioxide in more depth.

In the present work we have carried out a systematic and careful X-ray line broadening diffraction study, based on simplified methods [5], on eight samples of metastable tetragonal zirconia obtained at two different temperatures ( $1000$  and  $1050^\circ\text{C}$ ) for four isothermal crystallization times (1, 2, 4 and 8 h). Our aim was to establish the first, the presence and the amount of microstrains as well as their possible evolution; second, the average crystallite size and its growth as a function of the isothermal devitrification times.

The simplified X-ray line broadening methods use an integral breadth analysis of the "pure" X-ray diffraction lines obtained after appropriate corrections are carried out on the basis of suitably assumed line profile. Lattice constants for all the samples have also been determined in order to establish whether a cubic crystalline form may grow at the beginning of the devitrification process. Since it was hypothesized [6, 7] that microcrystalline zirconia can be present in a cubic metastable structure before reaching the tetragonal one, two more samples annealed at  $970^\circ\text{C}$  for 2 and 4 h have been analysed.

A Stokes-Fourier profile analysis on the previously mentioned samples will be reported elsewhere [8].

## 2. Experimental procedures

### 2.1. Sample preparation

The glass matrix of composition  $45\text{Al}_2\text{O}_3\text{-}37\text{ZrO}_2\text{-}17\text{SiO}_2\text{-}1\text{Na}_2\text{O}$  wt% was prepared from aluminium, zirconium, silicon and sodium alkoxides dissolved in an ethanol-methanol solvent mixture which was homogenized by stirring and mildly heating according to previously published methods [1, 2]. After exposure to the atmosphere for several hours, a gel formed which was slowly heated to eliminate the solvent and radicals which developed during mixture decomposition. Roy [9] hypothesized that in this kind of reaction the glass is formed from the parent alkoxides through a continuous process involving metastable phases.

The glassy material, heated up to  $900^\circ\text{C}$ , was made up of small pieces having an average size of a few millimeters. The devitrification isotherms were chosen at  $1000$  and  $1050^\circ\text{C}$  for 1, 2, 4 and 8 h in order to study the evolution of the system

towards the tetragonal zirconia, without interference from other crystalline phases which begin to crystallize at higher temperatures. Two more samples were prepared at 970°C for 2 and 4 h to complete the lattice constants study of the metastable phase.

We have gently milled the glassy material and sieved the obtained powder between 200 and 300 meshes to avoid subsequent possible introduction of lattice disorder by grinding. Isothermal heating was carried out in a tubular laboratory furnace with the temperature maintained to within  $\pm 0.5^\circ\text{C}$ . After thermal treatment, the samples were quenched in air from the isotherm temperature.

## 2.2. X-ray diffraction procedures

We used a Philips powder diffractometer connected to a highly stabilized generator with an X-ray tube working at 2 kW. Ni-filtered  $\text{CuK}\alpha$  radiation ( $\lambda = 1.5418 \text{ \AA}$ ), Soller slits, a graphite focussing crystal to monochromatize the diffracted beam, and a xenon-filled proportional counter were employed. The X-ray diffraction patterns were continuously recorded on a chart under the following experimental conditions: equatorial divergence slit  $\gamma = 1^\circ$ , receiving slit  $\nu = 0.2^\circ$ , time constant  $\text{RC} = 4 \text{ sec}$ , scanning velocity  $\omega = 0.5^\circ \text{ min}^{-1}$ . Under these conditions the so-called accuracy index for the peak intensity is equal to 1.6% [5]. From the obtained powder patterns the angular position for all peaks was established with an accuracy of  $\pm 0.02^\circ$  for  $2\theta$ , after calibrating the goniometer using the diffraction lines of a polycrystalline silicon disc with a lattice constant of  $a = 5.43054 \text{ \AA}$  [10].

The line broadening study was carried out by recording on a chart the 111 and 222 lines with a scanning velocity,  $\omega = 0.125 \text{ min}^{-1}$ , using a much lower sensitivity value for the weak 222 lines than for the other lines ( $I_{111} = 100$  and  $I_{222} = 5$  on a relative scale). The previously mentioned experimental conditions were kept constant. Obviously, the higher amplification used for 222 lines give rise to higher spurious fluctuations of the profiles, which were graphically smoothed out for the integral breadth determination. The intensity standard deviation now equals 0.8%. It is worth noting that a tail of the 222 line slightly overlaps a tail of the nearby 131 line this loss of information has been overcome by symmetrizing the 222 line which appears to be

symmetrical in a sufficiently large angular interval, where it is isolated from other adjacent lines.

As a reference sample for the instrumental and the  $K\alpha_1$ – $K\alpha_2$  doublet broadening corrections we used the same silicon disc employed for the angular calibration: for this purpose 111 and 311 reflection were recorded under the same experimental conditions already used in the case of zirconia. They were sufficiently narrow to ascribe their broadening to instrumental effects.

## 2.3. X-ray line integral breadth analysis: simplified methods

Rachinger correction [11] for the  $K\alpha_1$ – $K\alpha_2$  doublet broadening was performed for all the lines under study using graphical methods. Small  $2\theta$  intervals (one third of the corresponding  $\Delta\alpha_1$ – $\Delta\alpha_2$  angular separation) were used. The instrumental broadening was eliminated from the so obtained  $K\alpha_1$  components by means of the curve reported by Tekiz and Legrand [12], which was obtained using a square Cauchy profile function. This curve is close to that computed on the basis of a parabolic relation, [13], which is justified if the global broadening is considered as a result of convolution between a Gaussian pure profile and a Cauchian reference instrumental profile.

Actually, the  $K\alpha_1$  pure profiles of zirconia are intermediate between Gauss and Cauchy functions, while the silicon  $K\alpha_1$  profiles are of Cauchian type.

The integral breadth is defined as

$$\beta_i(2\theta) = \left( \int_{2\theta_1}^{2\theta_2} I(2\theta) d2\theta \right) / I_p(2\theta), \quad (1)$$

where  $I_p(2\theta)$  is the peak maximum intensity,  $2\theta_1$  and  $2\theta_2$  being the extremes of the  $K\alpha_1$  line under study.

The broadening due to crystallite size has been separated from the broadening due to microstrains using the following equation, valid for Cauchy/Gauss profile combinations [14]

$$\frac{1}{\beta_i(s) \cdot \bar{L}} = 1 - \frac{4e^2}{d_{hkl}^2 \cdot \beta_i^2(s)}. \quad (2)$$

The integral breadth of the pure diffraction profile  $\beta_i(s)$  is now expressed as a function of the reciprocal space variable  $s = 2 \sin \theta / \lambda$ ,  $e$  is an approximate upper limit for lattice distortions,  $\bar{L}$  is a

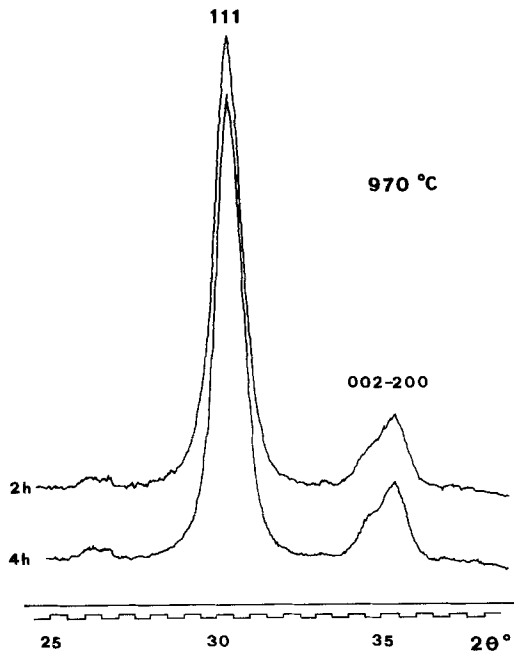


Figure 2 First three X-ray diffraction lines of the metastable tetragonal zirconia crystallized at 970 °C for 2 and 4 h. The 200–002 doublet is not separated, but appears to be clearly asymmetrical.

crystallite volume weighted mean size and  $d_{hkl}$  is the lattice spacing. If  $\bar{D}$  is the crystallite surface weighted mean, as given by Fourier methods, then for spherical particles the following equation is valid [15]

$$\bar{L} = \frac{\langle D^2 \rangle}{\langle D \rangle} = \frac{9}{8} \bar{D} = \frac{3}{4} D_0, \quad (3)$$

where  $D_0$  is the diameter of a single spherical crystallite.

It was shown by Buchanan *et al.* [16] that

$$e = 1.25 \langle \epsilon^2 \rangle^{1/2}, \quad (4)$$

where  $\langle \epsilon^2 \rangle^{1/2}$  is the rms microstrain calculated along the  $[hkl]$  crystallographic direction under study;  $e$  is defined by the relation  $e = (\Delta d/d)_{hkl}$ . It is clear that the solution of Equation 2, with respect to  $\bar{L}$  and  $e$ , requires lines of the same crystallographic family.

### 3. Results and discussion

Figs. 2 to 4 show the first three X-ray lines of the metastable tetragonal zirconia pattern for the samples devitrified at 970, 1000 and 1050 °C. It is possible to note that, by proceeding from the lowest isotherm (970 °C) to the highest one (1050 °C), and by increasing the heating time from

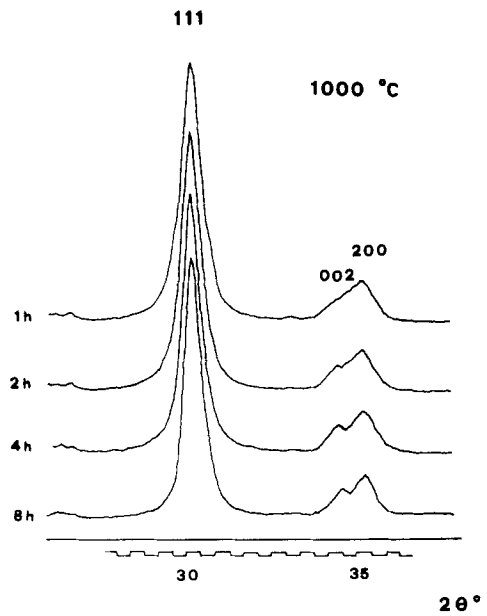


Figure 3 First three X-ray diffraction lines of the metastable tetragonal zirconia crystallized at 1000 °C for 1, 2, 4 and 8 h.

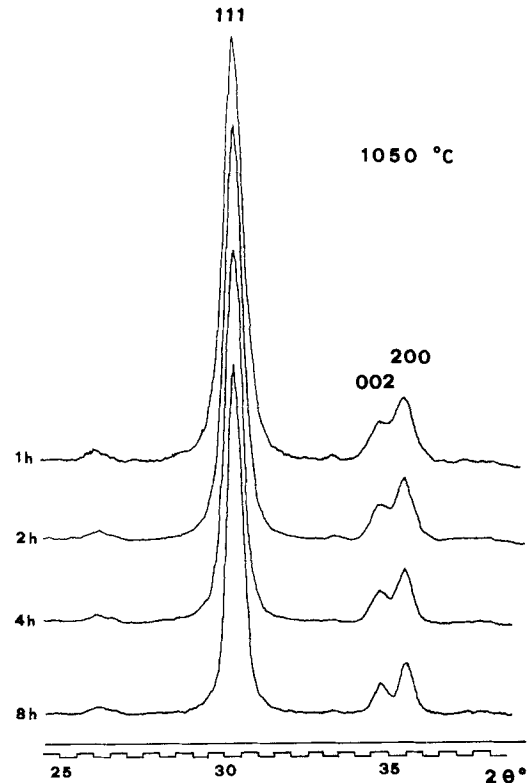


Figure 4 First three X-ray diffraction lines of the metastable tetragonal zirconia crystallized at 1050 °C for 1, 2, 4 and 8 h.

TABLE I Lattice constants  $a_0$  and  $c_0$  for the tetragonal unit cell of metastable  $ZrO_2$ . Literature data [4]  $a_0 = 5.0862 \pm 0.0005 \text{ \AA}$ ,  $c_0 = 5.1963 \pm 0.0005 \text{ \AA}$ , axial ratio  $c_0/a_0 = 1.0216$ .

Devitrification isotherm		$a_0(\text{\AA}) \pm 0.005$	$c_0(\text{\AA}) \pm 0.005$	Axial Ratio $c_0/a_0$
Temp ( $^{\circ}\text{C}$ )	time (h)			
970*	2	5.085	5.085	1.000
970*	4	5.085	5.085	1.000
1000*	1	5.085	5.085	1.000
1000	2	5.067	5.160	1.018
1000	4	5.089	5.180	1.018
1000	8	5.089	5.170	1.016
1050	1	5.092	5.182	1.018
1050	2	5.057	5.146	1.018
1050	4	5.082	5.179	1.019
1050	8	5.106	5.217	1.022

\*Pseudo-cubic unit cell.

1 to 8 h, 111 progressively gets narrower and the 002–200 doublet separates more.

On the basis of the angular position of all reflections measured between 20 and 65 $^{\circ}$  the  $a_0$  and  $c_0$  tetragonal lattice constants were calculated by means of a least square computer refining program. At higher  $2\theta$  angles, X-ray lines are too broad and weak for a precise  $d_{hkl}$  determination. Table 1 reports the lattice constants for the ten  $ZrO_2$  samples examined. For both samples devitrified at 970 $^{\circ}\text{C}$ , as well as for the sample devitrified

at 1000 $^{\circ}\text{C}$  for 1 h, the 002–200, 202–220 and 113–131 doublets could not be separated owing to their strong broadening. It was nevertheless necessary to assign a pseudo-cubic symmetry to these samples. However, the clear asymmetry shown by these apparent single lines confirms that a tetragonal lattice must be assigned to all the samples examined, even if masked by strong broadening effects.

Figs. 5 and 6 refer to the devitrification isotherms at 1050 $^{\circ}\text{C}$  for 1 h and at 1050 $^{\circ}\text{C}$  for 8 h and give examples of the broadened  $K\alpha_1$  profiles examined, after Rachinger correction. Fig. 7 shows the reference sample diffraction lines broadened only for instrumental reasons.

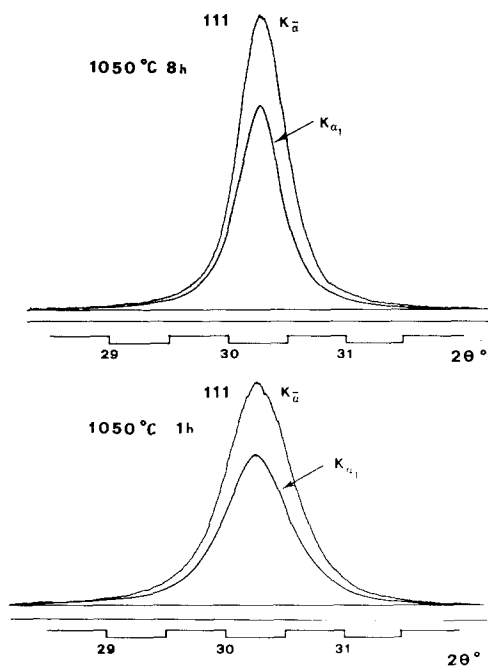


Figure 5 X-ray 111 peaks of the samples devitrified at 1000 $^{\circ}\text{C}$  (1 h) and at 1050 $^{\circ}\text{C}$  (8 h). The  $K\alpha_1$  profiles are also shown.

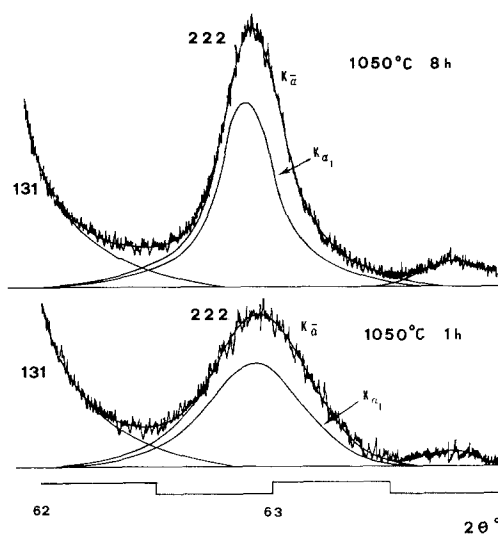


Figure 6 X-ray 222 peaks of the samples devitrified at 1000 $^{\circ}\text{C}$  (1 h) and at 1050 $^{\circ}\text{C}$  (8 h). The  $K\alpha_1$  profiles are also shown.

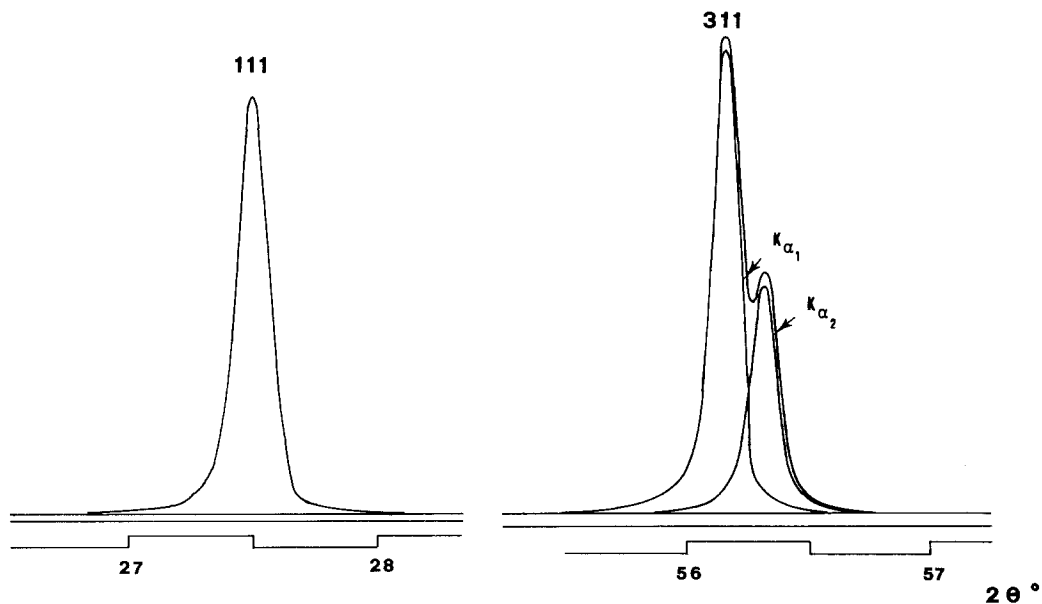


Figure 7 X-ray reference lines of polycrystalline silicon broadened only for instrumental reasons.

From the  $K\alpha_1$  diffraction pure profiles,  $\bar{D}$  and  $\langle \epsilon^2 \rangle^{1/2}$  were calculated using Equations 2 to 4. In Figs. 8 and 9, both parameters are plotted against the isotherm time for both the temperatures studied. First, it is important to note that microstrains are present in all samples: they are of the same order of magnitude as the microstrains present in cold-worked metals and alloys. The regularly increasing trend of  $\bar{D}$ , when devitrification time and/or temperature increase, is clearly shown by the plot of Fig. 8. In contrast, the trend of  $\langle \epsilon^2 \rangle^{1/2}$  with the annealing time is almost constant or slightly decreasing; while the values related to higher temperatures are systematically smaller.

Either from our repeatability tests or from

experimental data reported in the literature [17], the percentage error for a correlated series of samples may be estimated to be  $\pm 10\%$  for  $\bar{D}$  and  $\pm 20\%$  for  $\langle \epsilon^2 \rangle^{1/2}$ . The absolute accuracy may be estimated to be  $\pm 25\%$  and  $\pm 35\%$ , respectively.

As known [18], the most important source of error which might affect the X-ray line integral breadth is due to wrong layout of the background line. In order to evaluate this possible error, we have lowered, in a reasonable way, the background of the 222 lines of the three samples prepared at  $1050^\circ\text{C}$  with respect to the most reliable one. For the very intense, smooth and isolated 111 lines we have considered that the previously chosen background line could not be changed. The related percentage of lowering of the 222 peaks are

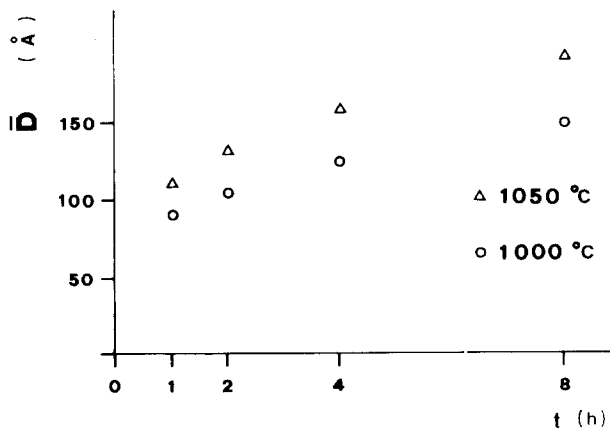


Figure 8 Plot of the average crystallite diameter along the [111] crystallographic direction,  $\bar{D}$ , versus the isothermal heating time for both temperatures studied ( $1000$  and  $1050^\circ\text{C}$ ).

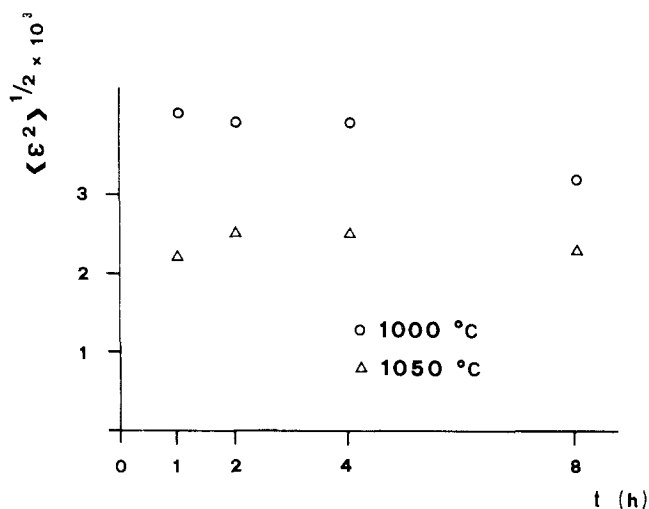


Figure 9 Plot of the rms microstrain along [111],  $\langle \epsilon^2 \rangle^{1/2}$ , versus the isothermal heating time for both temperatures studied (1000 and 1050° C).

reported in Table II, where all the values for  $\bar{D}$  and  $\langle \epsilon^2 \rangle^{1/2}$  are also indicated.

#### 4. Conclusions

The stabilization of the tetragonal  $\text{ZrO}_2$  pure phase obtained either by precipitation or by calcination at various temperatures up to 1000° C, was explained by Garvie [17] in terms of a higher surface energy for the stable monoclinic form with respect to that of the metastable, tetragonal one. In other words, according to Garvie, the tetragonal form cannot exist, at room temperature, for a crystallite size larger than 300 Å and he ascribed the stabilization, in terms of a contribution to the amount of free energy, to the surface energy of these very small tetragonal crystallites. Our present results confirm and enlarge this hypothesis in a more complicated system and at higher temperatures. In fact, we have found crystallite sizes smaller than 200 Å in our glass ceramic system up to 1050° C. We would probably arrive at analogous conclusions if we could increase the devitrification temperature

further without crystallizing our other phases. These phases are an obstacle in a careful study of X-ray line broadening.

Mitsuhashi *et al.* [19] report the presence of microstrains in only one sample of nearly pure tetragonal metastable  $\text{ZrO}_2$  produced from amorphous hydrated zirconium oxides precipitated from a zirconyl chloride solution with  $\text{NH}_3$  and subsequently heated at about 400° C. In their paper, the presence of lattice disorder was identified by a rough X-ray, half-maximum peak width analysis which uses the Hall equation [20] to separate crystallite size broadening from the broadening due to microstrains. This latter result is not completely convincing because no broadening due to microstrains was identified on the other three samples of metastable tetragonal  $\text{ZrO}_2$  examined by the above cited authors. Our present results clearly show a remarkable amount of microstrain, with average values ranging between 2 and  $4 \times 10^{-3}$ , in all the samples examined. The approximate constancy of these values with respect to the annealing time (see Fig. 9) is due to the absence of

TABLE II Average crystallite diameter and rms microstrain obtained by X-ray diffraction simplified methods for the metastable tetragonal zirconia isothermally annealed at 1000 and 1050° C

Devitrification isotherm		Final parameters		Parameters obtained by lowering the background line		Variation of the background line (%)
Temp (°C)	time (h)	$\bar{D}$ (Å)	$\langle \epsilon^2 \rangle^{1/2} \times 10^3$	$\bar{D}$ (Å)	$\langle \epsilon^2 \rangle^{1/2} \times 10^3$	
1000	1	91	4.0	—	—	—
1000	2	105	3.9	—	—	—
1000	4	115	3.9	—	—	—
1000	8	148	3.4	—	—	—
1050	1	111	2.2	117	3.9	-2
1050	2	132	2.5	145	4.6	-5
1050	4	156	2.5	158	3.2	-3
1050	8	192	2.3	—	—	—

relaxation effects. Therefore we believe that, in this case, microstresses cannot be related to a second phase and that they are probably cooling microstresses.

We also think that in our system, the free energy contributions due to both surface energy and strain field energy are the most important causes for metastable tetragonal  $ZrO_2$  stabilization. Besides, we cannot forget that a high content of amorphous  $Al_2O_3$  and/or  $SiO_2$  could enlarge the stabilization temperature range for the tetragonal  $ZrO_2$  [4]. Also, traces of water could help maintain the tetragonal form versus the monoclinic stable one, as recently shown by Murase and Kato in a phase transformation study of  $ZrO_2$  by ball-milling [21].

We determined lattice constants by l.s. methods since the beginning of zirconia crystallization. No X-ray diffraction cubic pattern has been observed. We believe in agreement with Garvie [17], that the observed strong line broadening effects can sometimes display a pseudo-cubic symmetry, even if in these cases a careful profile study could always give evidence of a clear asymmetry due to tetragonal doublets very close to each other.

### Acknowledgements

We thank the Italian Research Council (CNR) for financial support.

### References

1. G. CARTURAN, V. GOTTARDI and M. GRAZIANI, *J. non Cryst. Solids* **29** (1978) 41.
2. G. COCCO, G. FAGHERAZZI, G. CARTURAN and V. GOTTARDI, *Chem Commun.* (1978) 979.
3. V. GOTTARDI, R. DAL MASCHIO, G. MICHELOTTO and G. SCARINCI, *La Ceramica* **31** (1978) 47.
4. C. A. SORRELL and C. C. SORRELL, *J. Amer. Ceram. Soc.* **60** (1977) 495.
5. H. P. KLUG and L. E. ALEXANDER "X-ray Diffraction Procedures for Polycrystalline and Amorphous Materials" (J. Wiley & Sons, New York, (1974) pp. 271-418.
6. K. S. MAZDIYASNI, C. T. LYNCH and J. S. SMITH, *J. Amer. Ceram. Soc.* **49** (1966) 286.
7. G. KATZ, *ibid.* **54** (1971) 531.
8. G. FAGHERAZZI and G. ZARDETTO, *Gazz. Chim. Ital.* submitted.
9. R. ROY, *J. Amer. Ceram. Soc.* **52** (1969) 344.
10. K. E. BEU and D. L. SCOTT, USAEC Report GAT-T-1306, 1965.
11. W. A. RACHINGER, *J. Sci. Instrum.* **25** (1948) 254.
12. J. TEKIZ and C. LEGRAND, *Compt. Rend.* **261** (1965) 1247.
13. C. N. WAGNER and E. N. AQUA in "Advances in X-ray Analysis", Vol. 7 edited by W. M. Muller, G. R. Mallett and M. J. Fay. (Plenum Press, New York, 1964) pp. 46-65.
14. H. P. KLUG and L. E. ALEXANDER "X-ray Diffraction Procedures for Polycrystalline and Amorphous Materials" (J. Wiley & Sons, New York, 1974) pp. 618-708.
15. W. L. SMITH, *J. Appl. Cryst.* **5** (1972) 127.
16. D. R. BUCHANAN, R. L. McCULLOUGH and R. L. MILLER, *Acta Cryst.* **20** (1966) 922.
17. R. C. GARVIE, *J. Phys. Chem.* **69** (1965) 1238.
18. C. N. J. WAGNER in "Local Atomic Arrangements Studied by X-ray Diffraction" edited by J. B. Cohen and J. E. Hilliard. (Gordon Sci. Publ., New York, 1966) pp. 219-269.
19. T. MITSUHASHI, M. ICHIHARA and U. TATSUKE, *J. Amer. Ceram. Soc.* **57** (1974) 97.
20. W. H. HALL, *J. Instr. Metals* **75** (1949) 46.
21. Y. MURASE and E. KATO, *J. Amer. Ceram. Soc.* **62** (1979) 527.

Received 3 March and accepted 6 March 1980.